# Computational modeling of radiobiological effects in bone metastases for different radionuclides

**Francisco D. C. Guerra Liberal[a], Adriana Alexandre S. Tavares[b] and João Manuel R. S. Tavares[c]**

*Instituto de Ciência e Inovação em Engenharia Mecânica e Engenharia Industrial, Faculdade de Engenharia, Universidade do Porto, Rua Dr. Roberto Frias s/n, 4200-465 Porto, Portugal*

[a] meb12020@fe.up.pt

[b] adriana_tavares@msn.com

[c] tavares@fe.up.pt **(Corresponding author)**

## Running title: Computational modeling of radiobiological effects

**Name and Address for Correspondence:**

Prof. João Manuel R. S. Tavares

Faculdade de Engenharia da Universidade do Porto (FEUP)

Departamento de Engenharia Mecânica (DEMec)

Rua Dr. Roberto Frias, s/n

4200-465 PORTO

PORTUGAL

Telf.: +315 22 5081487, Fax: +315 22 5081445

**Email:** tavares@fe.up.pt Url: www.fe.up.pt/~tavares

# Computational modeling of radiobiological effects in bone metastases for different radionuclides


**ABSTRACT**

**Purpose:** Computational simulation is a simple and practical way to study and to compare a variety of radioisotopes for different medical applications, including the palliative treatment of bone metastases. This study aimed to evaluate and compare cellular effects modelled for different radioisotopes currently in use or under research for treatment of bone metastases using computational methods.

**Methods:** Computational models were used to estimate the radiation-induced cellular effects (Virtual Cell Radiobiology algorithm) post-irradiation with selected particles emitted by Strontium-89 ($^{89}$Sr), Samarium-153 ($^{153}$Sm), Lutetium-177 ($^{177}$Lu), and Radium-223 ($^{223}$Ra).

**Results:** Cellular kinetics post-irradiation using $^{89}$Sr $\beta^-$ particles, $^{153}$Sm $\beta^-$ particles, $^{177}$Lu $\beta^-$ particles and $^{223}$Ra $\alpha$ particles showed that the cell response was dose- and radio- nuclide-dependent. $^{177}$Lu beta minus particles and, in particular, $^{223}$Ra alpha particles, yielded the lowest survival fraction of all investigated particles.

**Conclusions:** $^{223}$Ra alpha particles induced the highest cell death of all investigated particles on metastatic prostate cells in comparison to irradiation with $\beta^-$ radionuclides, two of the most frequently used radionuclides in the palliative treatment of bone metastases in clinical routine practice. Moreover, the data obtained suggest that the used computational methods might provide some perception about cellular effects following irradiation with different radionuclides.



**Keywords:** Computational simulation; Radiation-induced effects; Radium-223; Lutetium-177; Bone metastases.

## I. INTRODUCTION

Cancer is a major public health concern, and it is associated with significant morbidity and mortality. In 2012, approximately 14 million new cases were diagnosed, and 8 million cancer-related deaths occurred (Stewart & Wild 2014). Prostate cancer is the second most common cancer in men worldwide (Stewart & Wild 2014). A large percentage of patients with prostate cancer (65-75%) develop bone metastasis (Chakraborty et al. 2008; Maini et al. 2003; Bedi et al. 2014), which often leads to severe pain, hypercalcemia, lack of mobility and depression that adversely affect these patients' life quality (Lewington 2005).

Bone metastasis occurs as a result of a complex pathophysiologic process between host and tumour cells leading to cellular invasion, migration adhesion, and stimulation of osteoclastic or osteoblastic activity. The process is mediated by parathyroid hormones, cytokines and tumour-derived factors (Tantivejkul et al. 2004; Roodman 2004; Roato 2013).

There are several therapeutic approaches targeting bone metastases and associated effects, including the use of analgesics, external beam radiotherapy and radionuclide systemic therapy. The latter, systemic palliative targeted-therapy with suitable radiopharmaceuticals, has emerged as a particularly appealing and efficient treatment modality for patients with multiple skeletal metastases (Maini et al. 2003; Pandit-Taskar et al. 2014; Silberstein 1996; Pillai et al. 2003).

Radionuclide therapy is characterized by reasonably selective delivery of therapeutic doses of radiation to systemically dispersed target tissues, with generally limited toxicity and few long-term side-effects (Unak 2002). Bone-seeking radiopharmaceuticals have considerable advantages, including convenience, ability to treat multiple metastatic lesions simultaneously, and the possibility of combination with chemotherapeutic agents for enhanced efficacy. The basis of successful radionuclide therapy relies on a high concentration and a prolonged retention of the radiopharmaceutical at the tumour site.

A major challenge associated with the palliative treatment of bone pain using selective radiopharmaceuticals is to deliver an adequate dose of ionizing radiation to the bone lesion, while minimizing the dose to healthy bone sites and adjacent tissues. In order or maximize the therapeutic effect and minimize normal-tissue irradiation, the radiation emitted by the targeted radionuclide should have an energy and tissue penetration range compatible with the volume of the lesion to be irradiated (Chakraborty et al. 2008; Wang et al. 2011). Therefore, studying the effects of particulate radiation at the cellular level is of interest to determine the suitability of a given radionuclide for target-tumor radiotherapy. There are essentially three main types of radioactive particles that are of interest for target-tumor radiotherapy: beta minus ($\beta^-$) particles, alpha ($\alpha$)

particles and Auger electrons. $\beta^-$ particles typically have a range of up to several millimeters in tissue, which may result in crossfire irradiation of cells adjacent to the targeted tumor. By contrast, α particles have a typical penetration range of less than 100 μm (Harrison et al. 2013). Auger electrons are low-energy electrons (typical energies around 20-100 keV) and have short penetration ranges only several nanometers to micrometers (Tavares & Tavares 2010). In addition to the physical properties of different radionuclides for target-tumor therapy, other characteristics should be taken into account while searching for the ideal radiopharmaceuticals for palliative treatment of bone metastases. For example, the radionuclide production costs and feasibility should be determined, and consideration should be given on whether its properties are amenable for radiochemistry procedures (Pillai et al. 2003). It is also important that the radionuclide to be used for palliative treatment of bone metastases allows for *in vivo* imaging, in order to assist with the determination of the suitable therapeutic dose to be used and to facilitate treatment monitoring (Henriksen et al. 2003; Pandit-Taskar et al. 2014).

In recent years, several reports have been published describing the use of Lutetium-177 ($^{177}$Lu) in the context of palliative treatment of bone metastases (Chakraborty et al. 2008; Abbasi 2012; Bryan et al. 2009; Yuan et al. 2013; Máthé et al. 2010; Abbasi 2011; Liberal et al. 2014; Pillai & Knapp 2015). Moreover, Strontium-89 ($^{89}$Sr), Samarium-153 ($^{153}$Sm) and Radium-223 ($^{223}$Ra) have already been approved by the Food and Drug Administration (FDA). The main physical characteristics of these radionuclides are indicted in Table I.

**< Table 1 should be inserted around here >**

$^{32}$P was the first radioisotope to be evaluated for palliative treatment of bone metastases and its first clinical use dates back to 1941 (Bouchet et al. 2000). Presently, one of the most commonly used radionuclides for palliative treatment of bone metastases in routine clinical practice is $^{153}$Sm, which was approved by the FDA for clinical use in 1997 (Sartor 2004). $^{89}$Sr is also currently used in the clinical setting for alleviation of bone pain and it was approved by the FDA for clinical use in 1993 (Das et al. 2009). Recently, a significant amount of work has been carried out using $^{223}$Ra, a promising therapeutic agent for palliative treatment of bone metastases, in order to take advantage of the short tissue penetration range associated with its emitted α particles. In clinical studies, $^{223}$Ra has demonstrated a highly significant improvement on patient overall survival, with mild side effects owing to its localized tissue penetration (2-10

cells). Its clinical use was approved by the FDA in 2013 (Harrison et al. 2013). Another promising radionuclide recently proposed for palliative treatment of bone metastasis was $^{177}$Lu due to its appealing physical characteristics, in particular its half-life of 6.73 days, gamma ray emission of 113keV (6.4%) and 208 keV (10.4%) and tissue penetration of 1.8 mm (Pillai et al. 2003; Dash et al. 2015).

There is now sufficient evidence of the importance of bystander effect that can modify the biology of the un-irradiated cells, and have a strong impact on therapeutic efficacy (Boyd et al. 2006). Bystander effect will be in addition to the direct effects of radiation exposure; therefore, its contribution must also be taken into account. Incorporation of a bystander effect model could have profound implications on the design of radionuclide protocols (Prise & O'Sullivan 2009). However, *in vivo* experiments to investigate the bystander response in radionuclide therapy are far more challenging than *in vitro* or *in silico* experiments. Consequently, computational simulation may be used to study and to compare a variety of radioisotopes for different medical applications, including the palliative treatment of bone metastases, under the same investigation conditions and might provide some insight into the bystander effect. However, radiation-induced effects are not yet fully understood, and regularly, new knowledge is added, consequently modelling cellular responses to irradiation is complex and challenging.

The Virtual Cell (VC) algorithm is an ongoing effort that aims to understand tumor pathogenesis and treatment. Results from in silico testing using the VC simulator, relies on multiscale modelling that have been tested against a total of 23 *in vitro* datasets obtained using different cell types and exposure conditions. Results from that *in silico* versus *in vitro* comparison demonstrated that the simulated data obtained using the VC algorithm compared favorably with real-life measured data, so it is widely used by scientific community in few research articles (Liberal et al. 2014;. Tavares & Tavares 2010).

This study aimed to use computational methods to evaluate and compare cellular effects modelled for different radioisotopes currently in use or under development for the palliative treatment of bone metastases, with regard to better understand the mechanisms that contribute to cell killing in each radionuclide at a wide range of absorbed doses and exposure time. Additionally, to infer how different outcomes, as mutagenic and genetic instability, neoplastic transformation and average number of direct lethal damage, relate to cell killing mechanism and no-direct effects, with special concern of bystander effect. In particular, the data reported here are focused on the bone metastases from the prostate carcinoma, given this is one of the most common types of cancer in men worldwide and the majority of these patients develop bone metastases.

## II. METHODS

The VC radiobiology simulator, was developed by Stewart and co-workers (Semenenko & Stewart 2004), to evaluate the following cellular endpoints: cell death, neoplastic transformation, chromosome aberration yields, induction of genomic instability, cell cycle kinetics and the probability of tumour eradication following radiation therapy.

Previous studies have shown that the $^{223}$Ra and $^{177}$Lu radiations induce the greatest number of deoxyribonucleic acid (DNA) lesions among all those investigated, with the lowest probability of correct repair of such lesions and the highest of induction of double-strand breaks (DSB) (Liberal et al. 2014).

The Monte Carlo damage simulation (MCDS) algorithm was used to obtain the number DSB and the fraction of complex DSB (FCB) (Semenenko & Stewart 2004; Semenenko et al. 2005) for $^{89}$Sr, $^{153}$Sm, $^{177}$Lu, $^{223}$Ra. The MCDS simulator is a fast Monte Carlo algorithm that models the damages to DNA by different particles and captures the major trends in the DNA damage spectrum predicted using detailed track structure simulations (Semenenko & Stewart 2004). The results obtained from the MCDS simulator (DSB and FCB) that yield the number of lesions caused by the radioactive particle to the DNA per Gy per cell were then applied as input parameters for the two-lesion kinetics (TLK) model used on the VC simulator. The approximate values of DSB and FCB obtained from the MCDS simulator for the evaluated particles were as follow: $^{89}$Sr $\beta^-$ particles, DSB = 50.055 and FCB = 0.1303; $^{153}$Sm $\beta^-$ particles, DSB = 49.631 and FCB = 0.1314; $^{177}$Lu $\beta^-$ particles, DSB = 50.430 and FCB = 0.1338; $^{223}$Ra $\alpha$ particles, DSB = 130.338 and FCB = 0.4565. By inserting these parameters, required by the TLK model into the VC input file, the cellular exposure scenario modeled would mimic the isotope in close proximity to the cell nucleus. The TLK model was preferred over other radiation exposure models, such as the repair-misrepair model (RMR) and lethal-potentially lethal model (LPL), as it applies an improved correlation between the biochemical processes of DSB and cell death, by subdividing DSB into simple or complex DSBs (Sach et al. 1997; Guerrero et al. 2002; Semenenko & Stewart 2004).

A comprehensive list with the input parameters used on the VC simulations is presented in the next section.

### II.A. Virtual Cell Simulator – Input Parameters

In this section, only the key VC input parameters used for the present study are discussed in detail, since an online platform, including a comprehensive VC user guide, is freely available

(http://faculty.washington.edu/trawets/vc).

The cell kinetics model (CKM) used was the quasi-exponential cell kinetics model (QECK), as that is the only available option for the current version of the VC simulator. Nonetheless, by using a high peak cell density (KAP) value (such as the one used in the present study, i.e. 1.0E+38 cells/$cm^3$) and by selecting a small initial cell population (initial number of cells – N0 = 1000 cells) compared to KAP×VOL (where VOL = tissue volume = 1 $cm^3$), the cell growth kinetics model becomes exponential. Furthermore, as the size of the cell population increases, the net cell birth rate decreases so that the cell population size approaches the asymptotic value KAP×VOL.

A cell type was evaluated: human metastatic prostate cells (TPOT – cell doubling time = 54 days; TC – cell cycle time = 48 hours) (Berges et al. 1995). The evaluated populations were set to be quiescent (GF – growth fraction = 0) and all cells are cycling (GF = 1) in order to understand the radiobiological effects from the nuclides.

The expected number of DSBs endogenously formed per cell-hour was defined as 4.3349E-03 $Gy^{-1}$ $cell^{-1}$. The values of the biophysical parameters: repair half-time (RHT), pairwise damage interaction rate (ETA) and probability of correct repair (A0), were set according to the requisites of the selected damage repair model. For example, the used TLK model sets the RHT, ETA and A0 values at certain intervals, including those described in Table 1. The probability of misrejoined DSB being lethal (PHI) and the fraction of residual damage at the end of the simulation that is treated as lethal (FRDL) are adjustable parameters. The absolute residual damage cutoff (ACUT) value is also an adjustable parameter, and it terminates the simulation when the amount of unrepaired residual damage is less than the specified value. Residual damages include radiation-induced DNA damages that remain unrepaired due to (1) DNA damage that was too severe, (2) presence of damages in inaccessible parts of the genome, (3) induction of damages during critical points in the cell cycle or (4) DNA damages converted into large DNA deletions (McMillan 1992). It is reasonable to accept that after a certain level of residual damages, any further cellular killing can be neglected as non-radiation related. The ACUT value of $1.0\times10^{-9}$ expected number of DNA damages per cell was chosen based on the fact that it should be smaller than the spontaneous endogenous damages (established to be in the order of $10^{-3}$) and a value of zero would not terminate the simulation, since ACUT was the only simulation control parameter adopted in the present study. The fraction of binary-misrepaired damages that are lethal (GAM) was set at 0.25, because according to Sach and co-workers, around 1/4 of the chromosome aberrations formed through the pairwise interaction process are lethal (i.e., GAM = 0.25) (Sach et al. 1997).

The selected radiation exposure scenario was the exponentially decreasing dose rate (DECAY), since the present work aimed at modeling the cellular responses to different absorbed doses delivered by internal targeted radiotherapy using 4 radioisotopes: $^{89}$Sr, $^{153}$Sm, $^{177}$Lu and $^{223}$Ra. For each radioisotope investigated, a radioactive constant (LAM) and a radionuclide half-life (RHL) was set according to the well-known decay scheme of these radioisotopes. The average background absorbed dose rate on planet Earth (BGDR) has been quantified as $2.73748\times10^{-7}$ Gy/h by the United Nations Scientific Committee on the Effects of Atomic Radiation (UNSCEAR) 2007 report (United Nations 2007). Irradiation periods of 2, 24, 48, 120 and 240 hours (TCUT – time allowed for repair after exposure) with total absorbed doses delivered to the cell population over all time (TAD) of 0.1, 0.5, 1, 2, 5 and 8 Gy were modeled using the VC simulator. The effective dose delivered to the cell system in a finite time interval (SAD) (0, TCUT), that is the SAD parameter is related to the TAD parameter by: SAD = (1-DCUT)×TAD, where DCUT = the dose cutoff used to truncate dose rate function after fraction 1-DCUT of total dose has been delivered. The DCUT is an adjustable parameter of the VC simulator and in this study it was set at 0.01, which means that the dose rate is truncated only after 99% of the set effective dose (SAD) has been delivered. This meant that SAD ≈ TAD. The use of the DCUT parameter is justifiable since at a given point, the activity of the radiation source becomes so small that any further radiation killing of the cell population can be neglected. The time to execute a DECAY simulation tends to increase as the number of steps increases. It is possible to control that by using the step-size tolerance (STOL) parameter, which typically ranges from about 0.05 to $1.0\times10^{-3}$ Gy/h. As the STOL value decreases, the time requested to perform the simulation increases and thus a compromise between time and accuracy must be made. In the present study, a STOL value of 0.01 Gy/h was used.

**II.B. Data analysis**

The VC data were expressed as the number of direct lethal damages per surviving cell, estimated number of surviving cells, probability of mutagenesis and enhanced genetic instability per surviving cell, neoplastic transformation frequency per irradiated cell and neoplastic transformation frequency per surviving cell. Data differences among the investigated radioisotopes were analyzed using the analysis of variance (ANOVA) statistical test, where $p < 0.01$ was considered statically significant.

**III. RESULTS**

The cell survival fraction results obtained after irradiation with different radionuclides and particles are shown

in Fig. 1. The estimated survival fraction rank order of all investigated particles was as follows: $^{89}$Sr $\beta^-$ particles > $^{153}$Sm $\beta^-$ particles > $^{177}$Lu $\beta^-$ particles >> $^{223}$Ra $\alpha$ particles. Additionally, statistically significant differences were observed among the different irradiating agents ($p < 0.0001$, ANOVA) Moreover, statistical analysis revealed no differences among the results obtained for $\beta^-$ particles, when the $^{223}$Ra $\alpha$ particles data was excluded ($p = 0.0252$, ANOVA).

**< Figure 1 should be inserted around here >**

The estimated number of metastatic prostate cells that survived irradiation when all cells were quiescent and when all cells were actively dividing is presented in Figs. 2a and 2b, respectively. When all cells were quiescent, the estimated number of surviving cells is lower than the estimated number, for actively dividing cellular populations, for the same exposer conditions (Figs. 2a and 2b). Statistically significant differences were observed among these four different irradiating agents when metastatic prostate cells were quiescent and all cells were actively dividing ($p < 0.0001$, ANOVA).

**< Figure 2 should be inserted around here >**

Figure 3 shows the mutagenesis and enhanced genetic instability probability per surviving cell for different irradiating sources. The analysis of these data reveals that the probability of mutagenesis and enhanced genetic instability of the cell population following irradiation with $\beta^-$ particles ($^{89}$Sr, $^{153}$Sm, $^{177}$Lu) increased with the increase in absorbed doses, with exception for high absorbed doses (8.0 Gy) for short periods of time ($\leq$ 24 h). On the other hand, the probability of mutagenesis and enhanced genetic instability of the cell population following irradiation with $^{223}$Ra $\alpha$ particles increased with the increase in exposure time and absorbed dose for values from 0.1 to 2 Gy; for absorbed doses higher than 2 Gy, the probability of mutagenic and enhanced genetic instability is negligible. Statistical analysis of the whole irradiation range reveals no differences among the results obtained with the different investigated particles ($p = 0.534$, ANOVA).

**< Figure 3 should be inserted around here >**

The neoplastic transformation frequency per irradiated cell and per surviving cell for each evaluated particle are shown in Figs. 4a and 4b, respectively. The probability of neoplastic transformation per irradiated cell was highest for lower doses, regardless of the radioactive particle used, and reduced as the dose increased (Fig. 4a). Conversely, the probability of neoplastic transformation frequency per surviving cell was lowest for low absorbed doses and increased as the absorbed dose increased for $^{223}$Ra α particles and constant whole irradiation range for $\beta^-$ particles ($^{89}$Sr, $^{153}$Sm, $^{177}$Lu) (Fig. 4b). The reduction rates of neoplastic transformation frequency per irradiated cell varied for low- and high-LET (linear energy transfer) particles, where the steepest reduction was observed for high-LET particles, and a slower reduction was found for low-LET particles. Statistically significant differences were observed among distinct radioactive particle neoplastic transformation frequencies per irradiated cell ($p < 0.0001$, ANOVA).

**< Figure 4 should be inserted around here >**

Finally, Fig. 5 shows the number of direct lethal damages per surviving cell as a function of absorbed dose. The results showed a rapid increase in cellular lethal damages as the absorbed dose increased for all the exposed periods tested, and statistically significant differences were observed among the results using distinct particles ($p = 0.002$, ANOVA).

**< Figure 5 should be inserted around here >**

## IV. DISCUSSION AND CONCLUSION

The results showed that the cell survival fraction decreased as a function of absorbed dose and increases as function of exposure time. The $^{223}$Ra α particles had the lowest survival fraction of all investigated irradiating agents in all irradiation scenarios, suggesting that these irradiating agents would be more promising in the killing of metastatic cells than the other investigated irradiating agents (Fig. 1). Moreover, that the cell response appears to behave in a LET and dose dependent manner

To further clarify the nature of the cell response following irradiation with different particles, three cellular endpoints were assessed by computational simulation mutagenesis and enhanced genetic instability per surviving cell (Fig. 3), neoplastic transformation per irradiated or surviving cell (Fig. 4) and number of direct lethal damages per surviving cell (Fig. 5). Cellular endpoints are usually associated with the bystander

effect (Lyng et al. 2002; Mothersill & Seymour 2003; Nagasawa et al. 2003; Prise & O'Sullivan 2009).

Our findings, obtained by means of computational simulators, indicated that the most promising agent for palliative treatment of bone metastases from prostate cancer is the $^{223}$Ra α particles that offer a therapeutic advantage over the $\beta^-$ radionuclides due to the higher capacity of inducing lethal damage and greater bystander effect at low-to-moderate doses. Other commonly used radioisotopes for palliative treatment of bone metastases, such as $^{89}$Sr, were found to be inferior in inducing lethal damages than $^{177}$Lu or $^{223}$Ra.

Detailed analysis of the cellular kinetics post-irradiation using $^{89}$Sr $\beta^-$ particles, $^{153}$Sm $\beta^-$ particles, $^{177}$Lu $\beta^-$ particles and $^{223}$Ra α particles showed that the cell response was dose- and radio- nuclide-dependent. For short TCUTs (≤ 48 h), virtually no differences were found between all $\beta^-$ particles. Conversely, for long TCUTs (≥ 120 h) on metastatic populations at low absorbed doses (0.1 and 0.5 Gy) all radiation sources tested were equivalently able to induce cell death. And at high-absorbed doses (≥1 Gy), irradiation with $^{223}$Ra α particles resulted in a lower number of surviving cells followed by $^{153}$Sm $\beta^-$ particles, $^{177}$Lu $\beta^-$ particles and $^{89}$Sn $\beta^-$ particles.

Our findings also showed that a larger number of actively dividing cells survived irradiation when compared with quiescent cells. This observation highlights the influence of cell kinetics on cell response to irradiation. We hypothesize that due the shorter doubling time (54 days) of metastatic prostate cells the unaffected cells were able to compensate radiation-induced damage by rapid cell duplication when all population were actively dividing.

Mutagenesis and enhanced genetic instability results showed that there is a non-linear relationship between genomic instability and absorbed dose (Fig. 3). Sokolov and co-workers in 2005, using primary human fibroblasts, found that for doses of alpha particles and gamma rays between 0.2 and 0.6 Gy, the number of DSB sites in bystander cells was higher than for doses of 2.0 Gy (Sokolov et al. 2005). DNA DSBs have been associated with genetic instability, which is one of the mechanisms underlying the bystander effect. Moreover, Boyd and co-workers in 2006, showed dose-response relationship for the indirect effects produced by cellular exposure with low-LET $\beta^-$ radionuclides, using human glioma cells and human bladder carcinoma cells (Boyd et al. 2006). The results from the VC simulator showed that the probability of mutagenesis and genetic instability for $^{223}$Ra α particles was higher for doses ranging between 0.1 and 1 Gy than for doses equal to or above 2 Gy (Fig. 3). These findings seem to be in line with in vitro observations reported by Sokolov and co-workers in 2005 (Sokolov et al. 2005) and Boyd and co-workers in 2006 (Boyd et al. 2006).

The data also showed that the probability of cell transformation per irradiated cell was higher for lower absorbed doses (Fig. 4a), while the probability of cell transformation per surviving cell (Fig. 4b), and the number of direct lethal damages per surviving cell (Fig. 5) was higher for high absorbed doses. Redpath and co-workers studies have also reported that the cell transformation frequency per surviving cell increased with increasing absorbed doses (Redpath & Elmore 2007; Redpath 2006). Results from the VC simulator are in line with these prior observations. The increasing probability of cell transformation per surviving cell with increasing absorbed doses means that the normal cells surrounding the tumor have to be protected when performing target tumor radiotherapy, particularly for high doses of radiation.

Taken all together, the data show that, at the lower absorbed doses, the transformation frequency per irradiated cell when exposure with an $\beta^-$ emitter radionuclide and genetic instability of surviving cells when exposure to an α emitter radionuclide are major contributors for the low number of estimated surviving cells, since the values of direct lethal damages and transformation frequency per surviving cell for lower doses are small compared with higher absorbed doses. Conversely, at higher absorbed doses, cell death is mainly related to the number of direct lethal damages, the transformation frequency per surviving cell and the radiation quality. This does not mean that genetic instability of surviving cells and transformation frequency per irradiated cell effects have no relevance at higher doses, but that their relative importance as a portion of the total effect tends to decrease as the dose increases.

The data obtained from the VC simulator should be interpreted with caution due to the parameter estimation issues associated with mechanism-based radiation response models. Although flexibility in changing input parameters will have obvious advantages by allowing the modeling of multiple irradiation scenarios, it also represents an issue due to the uncertainty associated with the somewhat arbitrary choice of a certain value for a give parameter. Together with in vitro or in vivo studies data, simulators such as the one adopted in this work, would allow better experimental design and could be used to study different processes associated with cell response to ionizing radiation.

Computational simulation is widely recognized as an essential method to study the physics of radiobiology. Nevertheless, some limitations have been pointed out, including modeling and evaluation based on current knowledge, which works as a mechanistic process. Furthermore, the computational algorithms used in this study only model simple repair processes and exclude DSBs repair processes. Moreover, the used algorithms assume an optimal scenario of ionizing energy deposition directly into the DNA, scenario that often is challenging to achieve in vitro and in vivo due to inefficient radiopharmaceutical biodistribution

processes, and assume that the radioactivity was distributed uniformly throughout the target. However, there have been dramatic improvements in dosimetry models and simulators that reflect the substructure of target and elements within them (Vaziri et al. 2014). Consequently, future in vitro and in vivo studies are crucial to establish a definite role of the simulator used here and careful interpretation of the results is therefore recommended. Nevertheless, the comparative analysis of the VC generated data with prior studies support the use of the VC simulator as a useful tool in the field of radiobiology, with particular utility in the context of radiotherapy.

The radioisotopes studied included β emitters and α emitters, covering the most commonly used particles in current targeted tumor radiotherapy in bone metastases. Doses ranging between 0.1 and 8.0 Gy were tested on quiescent and actively dividing cell populations and the number of surviving cells following irradiation was estimated. The VC simulator is a user-friendly platform that provides output data consistent with experimental terminology used by cellular radiobiologists. This might foster the future use of the VC simulator by non-computer scientists, by using a similar approach as the one described here.

In conclusion, the data obtained using the VC simulator indicate that for doses below 0.1Gy all tested particles ($^{89}$Sr $\beta^-$ particles, $^{153}$Sm $\beta^-$ particles, $^{177}$Lu $\beta^-$ particles, $^{223}$Ra α particles) seem to be equally able to induce cell death independently of their LET. At low doses, cell death was found to be due to high genetic instability and cell transformation that are cellular end-points measured when investigating the bystander effect. On the contrary, at high-absorbed doses, cellular response to radiation seems to be dose and LET dependent.

$^{223}$Ra α particle emission is an appealing strategy for the treatment of bone micrometastases, owing to the short tissue range penetration associated with these radioactive particles that can allow for a more circumscribed irradiation surface. Furthermore, typically α emitters induce less hematologic toxicity for a given bone surface dose than $\beta^-$ emitters (Pandit-Taskar et al. 2014; Harrison et al. 2013; Nilsson et al. 2013). The high linear energy transfer of α particles has been associated with greater biological effectiveness than that of β− particles (Pandit-Taskar et al. 2014; Harrison et al. 2013; Nilsson et al. 2013). $^{223}$Ra-dichloride has been shown to not only have a palliative effect but also a survival prolonging effect (Harrison et al. 2013; Nilsson et al. 2013).

Among the $\beta^-$ particle emitters, the $^{177}$Lu has the lowest tissue penetration range (1.8 mm). A common concern associated with the use of $\beta^-$ particle is related to their relatively long range in tissue, which can result in energy deposition in neighboring, nontargeted cells, a phenomenon known as “cross-fire” that may

lead to excessive bystander effects. With α particle emitters, due to their short tissue penetration range, the cross fire effect is not such a concern, but may require targeting virtually every cell within large size tumors and does not take advantage of the positive bystander effects (Jackson et al. 2013). The relatively short range of $^{177}$Lu $\beta^-$ particles in tissues is at the lower end of the $\beta^-$ particle generally, thereby minimizing the potential adverse effects cross-fire often associated with $\beta^-$ particle emitters. Also, it is higher than typical α particles allowing us to take advantage of the positive bystander effects that are not attainable with conventional α particles emitters.

Notwithstanding, previously published data have shown that the $^{223}$Ra α particles have an increased antitumor effect when compared with $\beta^-$ particles (Nilsson et al. 2005; Pandit-Taskar et al. 2014; Nilsson et al. 2013). This might explain recent data demonstrating that $^{223}$Ra was the first agent in its class to show an overall survival advantage in patients with bone metastases from prostate carcinomas (Goyal & Antonarakis 2012). In line with these observations, our analysis showed a superiority of the $^{223}$Ra α particles compared with the modeled $\beta^-$ particles. In particular, the clinical outcome of a given therapeutic depends not only on the cellular response but also on, for example, the individual patient differences in clinical conditions, patient preparation, life-expectancy, age, and the existence of secondary tumors. Furthermore, radiopharmaceuticals biodistribution, elimination, and concentration in the biological target tissue in vivo would also impact therapeutic response.

In conclusion, this study compared different irradiating agents using the same exposure conditions and controllable cell populations to clarify the radiobiological effects of these radioisotopes for palliative treatment of bone metastases, specifically in the context of prostate cancer. The top agent able to induce the highest cellular damage and cell death was found to be the $^{223}$Ra α particles. $^{223}$Ra-dichloride is a particularly appealing approach for the treatment of bone metastases based on the data reported here, radionuclide physical properties, suitable production methods and feasible logistics of distribution. Within the β− particle emitters investigated, $^{177}$Lu was the preferred one due its adequate half-life and physical properties for image acquisition. There is much still to understand with regard to the differences biological processes that underpin the differences in behavior of high- and low-LET radionuclides. However, the data obtained suggest that the computational methods used might provide some insight into cellular effects following irradiation. Although, *in vitro* and *in vivo* data are necessary to support our findings and clarifies how much the contribution of the in lethality is owing to a direct effect and what component of it is owing to bystander effect for each radionuclide and scenario, the VC simulator can be useful as a first screening tool for predicting and

modelling cellular effects and the bystander effect due to the close association found between genetic instability, cell transformation and the bystander effect.

## CONFLICT OF INTEREST

The authors declare no conflict of interests regarding the publication of this paper.

## ACKNOWLEDGE

Authors gratefully acknowledge the funding of Project NORTE-01-0145-FEDER-000022 - SciTech - Science and Technology for Competitive and Sustainable Industries, cofinanced by "Programa Operacional Regional do Norte" (NORTE2020), through "Fundo Europeu de Desenvolvimento Regional" (FEDER).

This work was also supported by Fundação para a Ciência e Tecnologia (FCT-MCTES), Radiation Biology and Biophysics Doctoral Training Programme (RaBBiT, PD/00193/2012); UID/Multi/04378/2013 (UCIBIO); UID/FIS/00068/2013 (CEFITEC); and scholarship grant number SFRH/BD/11448/2016 to (FL).

## REFERENCES

Abbasi, I.A., 2012. Preliminary studies on (177)Lu-labeled sodium pyrophosphate (177Lu-PYP) as a potential bone-seeking radiopharmaceutical for bone pain palliation. *Nucl Med Biol*, 39(6), pp.763–9.

Abbasi, I.A., 2011. Studies on 177Lu-labeled methylene diphosphonate as potential bone-seeking radiopharmaceutical for bone pain palliation. *Nucl Med Biol,* 38(3), pp.417–25.

Bé, M. et al., 2008. Table of Radionuclides. *Bureau International des Poids et Mesures*, 1–6.

Bedi, M., King, D.M. & Tutton, S., 2014. Minimally Invasive Local Treatments for Bone and Pulmonary Metastases. *Minimally Invasive Surgery*, vol. 2014, article ID.719394.

Berges, R.R. et al., 1995. Implication of cell kinetic changes during the progression of human prostatic cancer. *Clin. Cancer Res.*, 1(5), pp.473–480.

Bouchet, L.G. et al., 2000. Considerations in the selection of radiopharmaceuticals for palliation of bone pain from metastatic osseous lesions. *J Nucl Med*, 41(4), pp.682–687.

Boyd, M. et al., 2006. Radiation-induced biologic bystander effect elicited in vitro by targeted radiopharmaceuticals labeled with alpha-, beta-, and auger electron-emitting radionuclides. *J Nucl Med*, 47(6), pp.1007–1015.

Bryan, J.N. et al., 2009. Comparison of systemic toxicities of 177Lu-DOTMP and 153Sm-EDTMP administered intravenously at equivalent skeletal doses to normal dogs. *J Nucl Med* Technol, 37(1), pp.45–52.

Chakraborty, S. et al., 2008. Comparative studies of 177Lu-EDTMP and 177Lu-DOTMP as potential agents for palliative radiotherapy of bone metastasis. *Appl Radiat Isot*, 66(9), pp.1196–1205.

Das, T. et al., 2009. (170)Tm-EDTMP: a potential cost-effective alternative to (89)SrCl(2) for bone pain palliation. *Nucl Med Biol*, 36(5), pp.561–568.

Dash, A., Pillai, M.R.A. & Knapp, F.F., 2015. Production of 177Lu for Targeted Radionuclide Therapy: Available Options. *Nucl Med Mol Imaging*, 49(2), pp.85-107.

Goyal, J. & Antonarakis, E.S., 2012. Bone-targeting radiopharmaceuticals for the treatment of prostate cancer with bone metastases. *Cancer Lett*, 323(2), pp.135–146.

Guerrero, M. et al., 2002. Equivalence of the linear-quadratic and two-lesion kinetic models. *Phys Med Biol*, 47(17), pp.3197–3209.

Harrison, M.R. et al., 2013. Radium-223 chloride: a potential new treatment for castration-resistant prostate cancer patients with metastatic bone disease. *Cancer Manag Res*, 5, pp.1–14.

Henriksen, G. et al., 2003. Targeting of Osseous Sites with alpha-Emitting 223Ra: Comparison witn the Beta-Emitter 89Sr in Mice. *J Nucl Med*, 44(2), pp.252–259.

Jackson, M.R., Falzone, N. & Vallis, K.A., 2013. Advances in Anticancer Radiopharmaceuticals. *Clinl Oncol*, 25(10), pp.604–609.

Lewington, V.J., 2005. Bone-seeking radionuclides for therapy. *J Nucl Med*, 46 Suppl 1, p.38S–47S.

Liberal, F.D.C.G., Tavares, A.A.S. & Tavares, J.M.R.S., 2014. Comparative analysis of 11 different radioisotopes for palliative treatment of bone metastases by computational methods. *Medl Phys*, 41(114101).

Lyng, F.M., Seymour, C.B. & Mothersill, C., 2002. Early events in the apoptotic cascade initiated in cells treated with medium from the progeny of irradiated cells. *Radiat Prot Dosimetry*, 99(1–4), pp.169–172.

Maini, C.L. et al., 2003. Radionuclide therapy with bone seeking radionuclides in palliation of painful bone metastases. *J Exp Clinl Cancer Res,* 22(4 Suppl), pp.71–4.

Máthé, D. et al., 2010. Multispecies animal investigation on biodistribution, pharmacokinetics and toxicity of 177Lu-EDTMP, a potential bone pain palliation agent. *Nucl Med Biol*, 37(2), pp.215–26.

McMillan, T.J., 1992. Residual DNA damage: What is left over and how does this determine cell fate? *Eur J Cancer*, 28(1), pp.267–269.

Mothersill, C. & Seymour, C., 2003. Radiation-induced bystander effects, carcinogenesis and models. *Oncogene*, 22(45), pp.7028–7033.

Nagasawa, H., Huo, L. & Little, J.B., 2003. Increased bystander mutagenic effect in DNA double-strand break repair-deficient mammalian cells. *Int J Radiat Biol*, 79(1), pp.35–41.

Nilsson, S. et al., 2005. First clinical experience with alpha-emitting radium-223 in the treatment of skeletal metastases. *Clin Cancer Res,* 11(12), pp.4451–9.

Nilsson, S. et al., 2013. Two-year survival follow-up of the randomized, double-blind, placebo-controlled phase II study of radium-223 chloride in patients with castration-resistant prostate cancer and bone metastases. *Clin Gentitourin Cancer*, 11(1), pp.20–26.

Pandit-Taskar, N., Larson, S.M. & Carrasquillo, J. a, 2014. Bone-Seeking Radiopharmaceuticals for Treatment of Osseous Metastases, Part 1: α Therapy with 223Ra-Dichloride. *J Nucl Med*, 55(2), pp.268–74.

Pillai, A.M.R. & Knapp, F.F.R., 2015. Evolving Important Role of Lutetium-177 for Therapeutic Nuclear Medicine. *Curr Radiopharm*, 8(2), pp.78–85.

Pillai, M.R. a. et al., 2003. Production logistics of 177Lu for radionuclide therapy. *Appl Radiat Isot*, 59(2–3), pp.109–118.

Prise, K.M. & O'Sullivan, J.M., 2009. Radiation-induced bystander signalling in cancer therapy. *Nat Rev Cancer*, 9(5), pp.351–360.

Redpath, J. & Elmore, E., 2007. Radiation-Induced Neoplastic Transformation in Vitro , Hormesis and Risk Assessment. *Dose Response*, 5(2), pp.123–130.

Redpath, J.L., 2006. Suppression of Neoplastic Transformation In Vitro by Low Doses of Low Let Radiation. *Dose Response*, 4(4), pp.302–308.

Roato, I., 2013. Interaction among cells of bone, immune system, and solid tumors leads to bone metastases. *Clinical & Developmental Immunology*, Vol(2013), article ID 315024.

Roodman, G.D., 2004. Mechanisms of bone metastasis. *N Engl J Med*, 350(16), pp.1655–64.

Sach, R.K., Hahnfeld, P., & Brenner, D.J., 1997. The link between low-LET dose-response relations and the underlying kinetics of damage production/repair/misrepair. *Int J Radiat Biol*, 72(4), pp.351–374.

Sartor, O., 2004. Overview of samarium Sm 153Llexidronam in the treatment of painful metastatic bone disease. *Rev Urology*, 6 (Suppl 10), pp.S3–S12.

Semenenko, V.A. & Stewart, R.D., 2005. Monte Carlo simulation of base and nucleotide excision repair of clustered DNA damage sites. I. Model properties and predicted trends. *Radiat Res*, 164(2), pp.180–193.

Semenenko, V. A & Stewart, R.D., 2004. A fast Monte Carlo algorithm to simulate the spectrum of DNA damages formed by ionizing radiation. *Radiat Res*, 161(4), pp.451–7.

Silberstein, E.B., 1996. Dosage and Response in Radiopharmaceutical Therapy of Painful Osseous Metastases J Nucl Med, 37(2), pp.249–252.

Sokolov, M. V et al., 2005. Ionizing radiation induces DNA double-strand breaks in bystander primary human fibroblasts. *Oncogene*, 24(49), pp.7257–7265.

Stewart, B.W. & Wild, C.P., 2014. *World Cancer Report 2014* C. P. Stewart, B. W., Wild, ed., IARC Nonserial Publication.

Tantivejkul, K., Kalikin, L.M. & Pienta, K.J., 2004. Dynamic process of prostate cancer metastasis to bone. *J Cell Biochem*, 91(4), pp.706–17.

Tavares, A.A.S. & Tavares, J.M.R.S., 2010. (99m)Tc Auger electrons for targeted tumour therapy: a review. *Int J Radiation Biol*, 86(4), pp.261–70.

Tavares, A.A.S. & Tavares, J.M.R.S., 2010. Evaluating 99mTc Auger electrons for targeted tumor radiotherapy by computational methods. *Med Phys*, 37(7), p.3551-9.

Unak, P., 2002. Targeted Tumor Radiotherapy. *Braz Arch Biol Technol*, 45, pp.97–110.

United Nations, 2007. Report of the United Nations Scientific Committee on the Effects of Atomic Radiation Report of the fifty-fifth session. Suplement 46.

Vaziri, B. et al., 2014. MIRD pamphlet No. 25: MIRDcell V2.0 software tool for dosimetric analysis of biologic response of multicellular populations. *J Nucl Med*, 55(9), pp.1557–1564.

Volkert, W. a & Hoffman, T.J., 1999. Therapeutic radiopharmaceuticals. *Chem Rev*, 99(9), pp.2269–92.

Wang, C. et al., 2011. In vitro study on apoptosis induced by strontium-89 in human breast carcinoma cell line. *J Biomed Biotechnol*, 2011, p.541487.

Yuan, J. et al., 2013. Efficacy and safety of 177Lu-EDTMP in bone metastatic pain palliation in breast cancer and hormone refractory prostate cancer : a phase II. *Clin. Nucl. Med.*, 38(2), pp.88–92.

**TABLE AND FIGURES**

**Table I:** Summary of main physical properties of different radionuclides in clinical use or under research for palliative treatment of bone metastases.

| Radionuclide | Emission Type | $E_{mean}$ (MeV) (%) | $E_\gamma$ (keV) (%) | $T_{1/2}$ (days) | Tissue penetration range (mm) | Auger Transition – Average Energy (keV) (%) | References |
|---|---|---|---|---|---|---|---|
| $^{89}Sr$ | $\beta^-$ | 0.5846 (99.99) | 909 (0.1) | 50.5 | 6.7 | ------- | (Bé et al. 2008; Lewington 2005; Volkert & Hoffman 1999) |
| $^{153}Sm$ | $\beta^-$ | 0.2253 (48.2) | 103 (28) | 1.93 | 3.4 | 34 (4.6) | (Bé et al. 2008; Lewington 2005; Volkert & Hoffman 1999) |
| $^{177}Lu$ | $\beta^-$ | 0.1494 (79.3) | 211 (11) | 6.2 | 1.8 | 6 (9) | (Bé et al. 2008; Volkert & Hoffman 1999) |
| $^{223}Ra$ | $\alpha$ | 5.71581 (45.6) | 154 (5.6) | 11.4 | 0.1 | 62 (1.7) | (Bé et al. 2008; Lewington 2005; Henriksen et al. 2003) |

Legend: $T_{1/2}$ (days) – radioisotope half-life in days; E (MeV) (%) – particle energy and respective decay abundance shown in parentheses; $E_\gamma$ (KeV) (%) – gamma ray energy and respective abundance in total energy emission shown in parentheses; Tissue penetration range (mm) – maximum tissue penetration in soft tissue shown in millimeters; Auger Transition – Average Energy (keV) (%) – average Auger transition energy and respective abundance shown in parentheses.

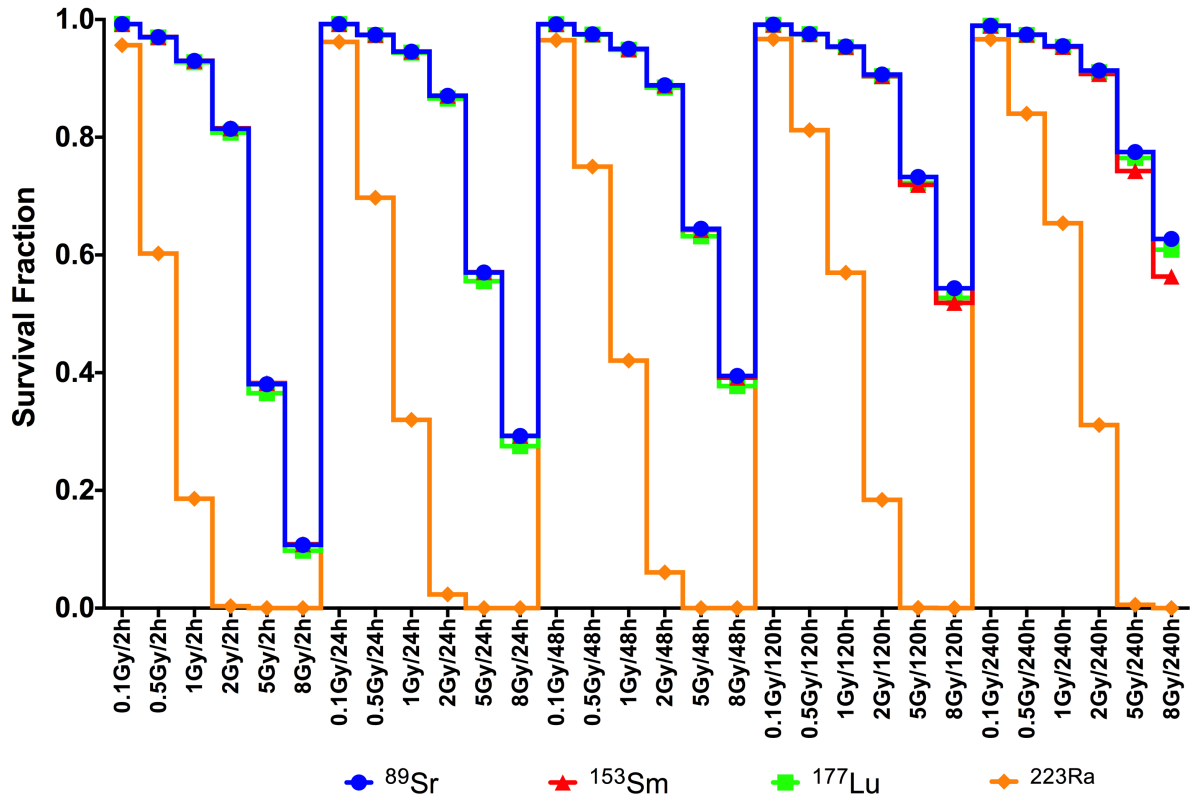


**Figure 1:** Cell survival fraction estimated for $^{89}Sr$, $^{153}Sm$, $^{177}Lu$ and $^{223}Ra$.

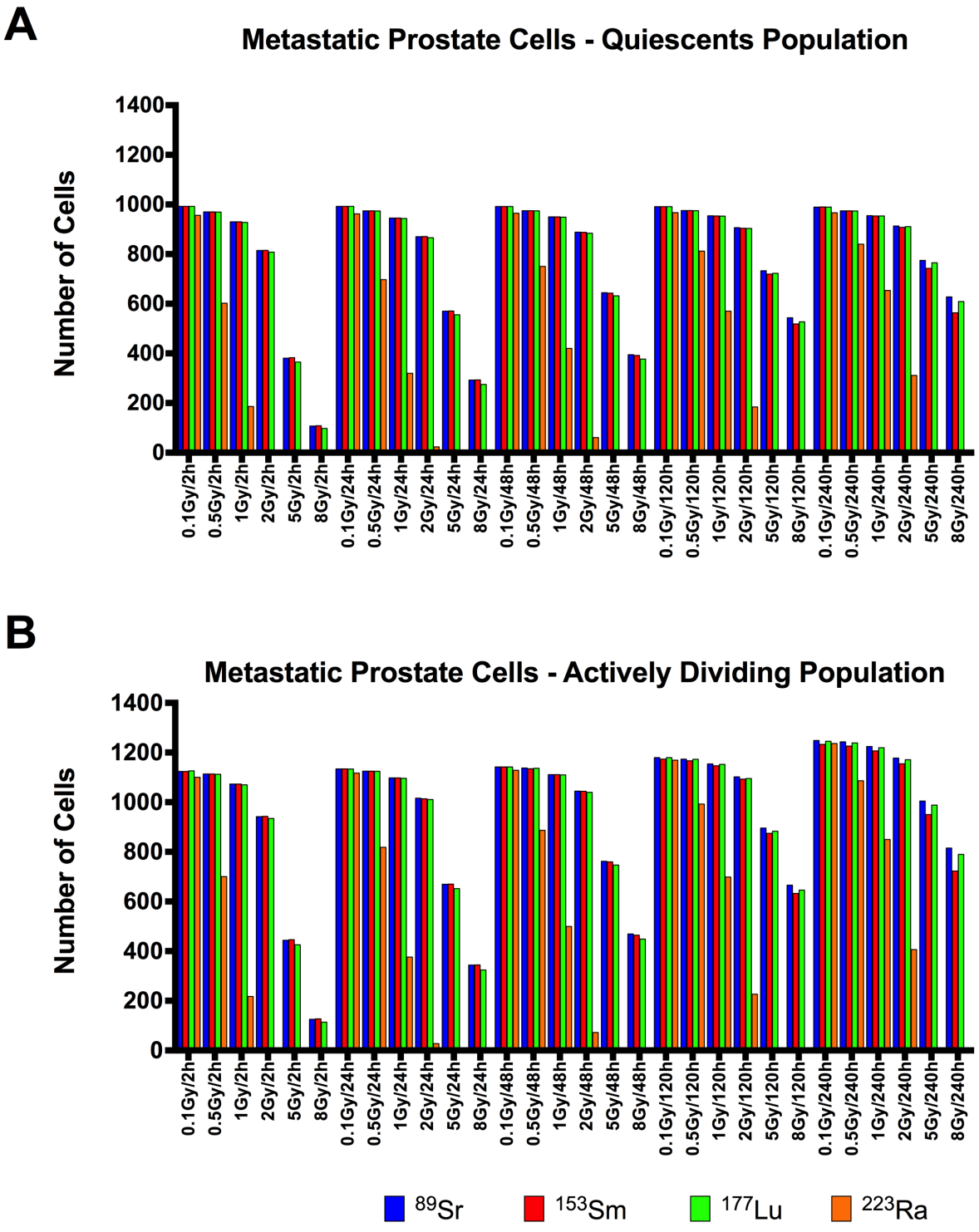


**Figure 2:** Number of metastatic prostate cells that survive irradiation with different irradiating agents in a quiescent cell population (a), and in cells actively dividing (b). (Simulated doses of 0.1, 0.5, 1, 2, 5, and 8 Gy and irradiation periods of 2, 24, 48, 120, and 240 h.)

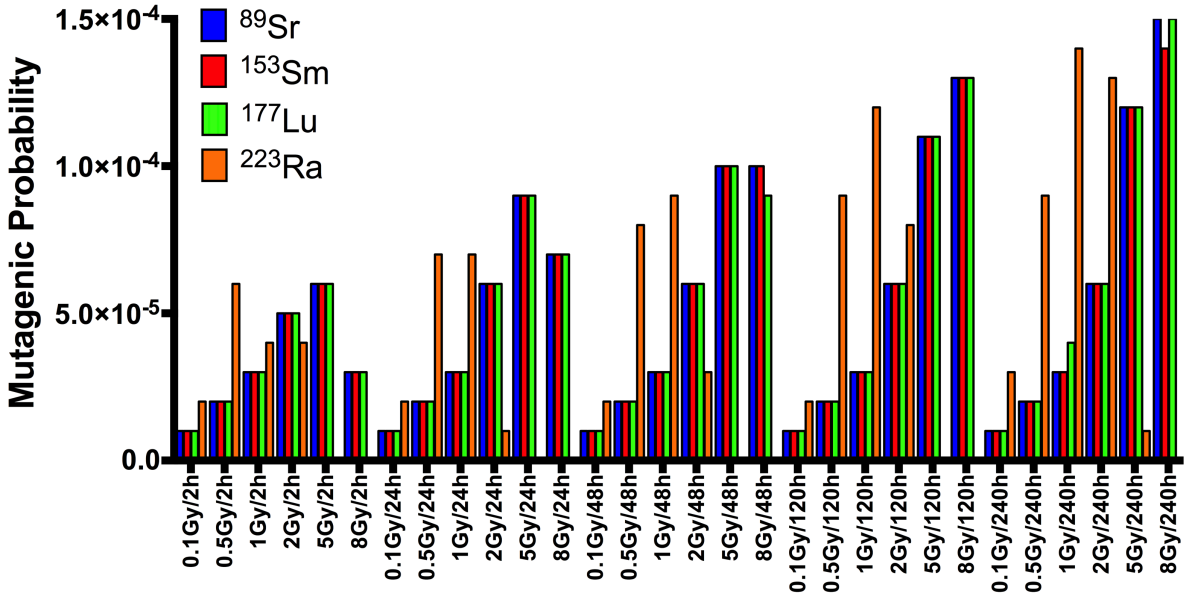


**Figure 3:** Mutagenesis and enhanced genetic instability probability per surviving cell for different irradiating sources: whole irradiation range.

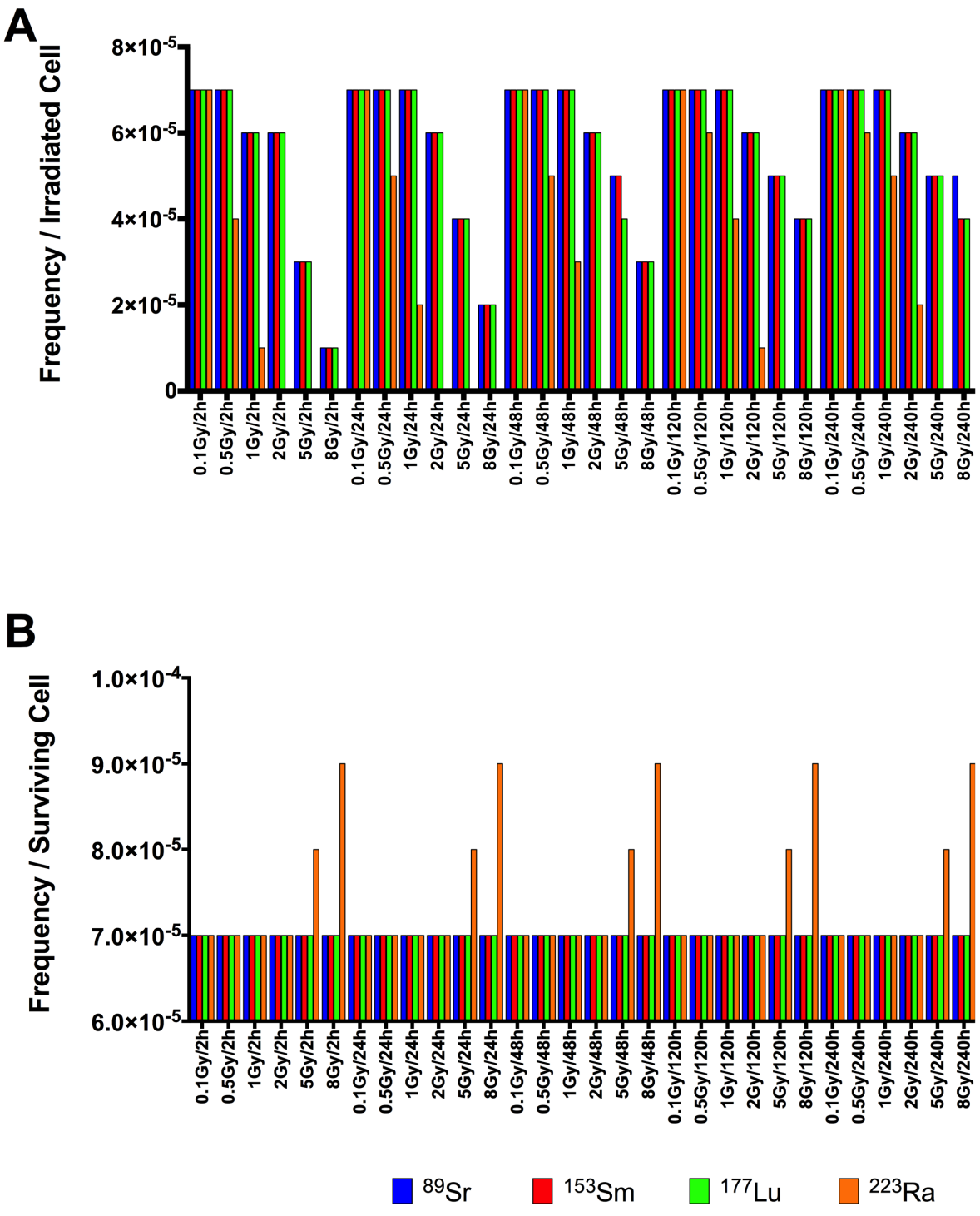


**Figure 4:** Neoplastic transformation frequency per irradiated cell (a) and per surviving cell (b), following exposure to different radiation sources and distinct absorbed doses.

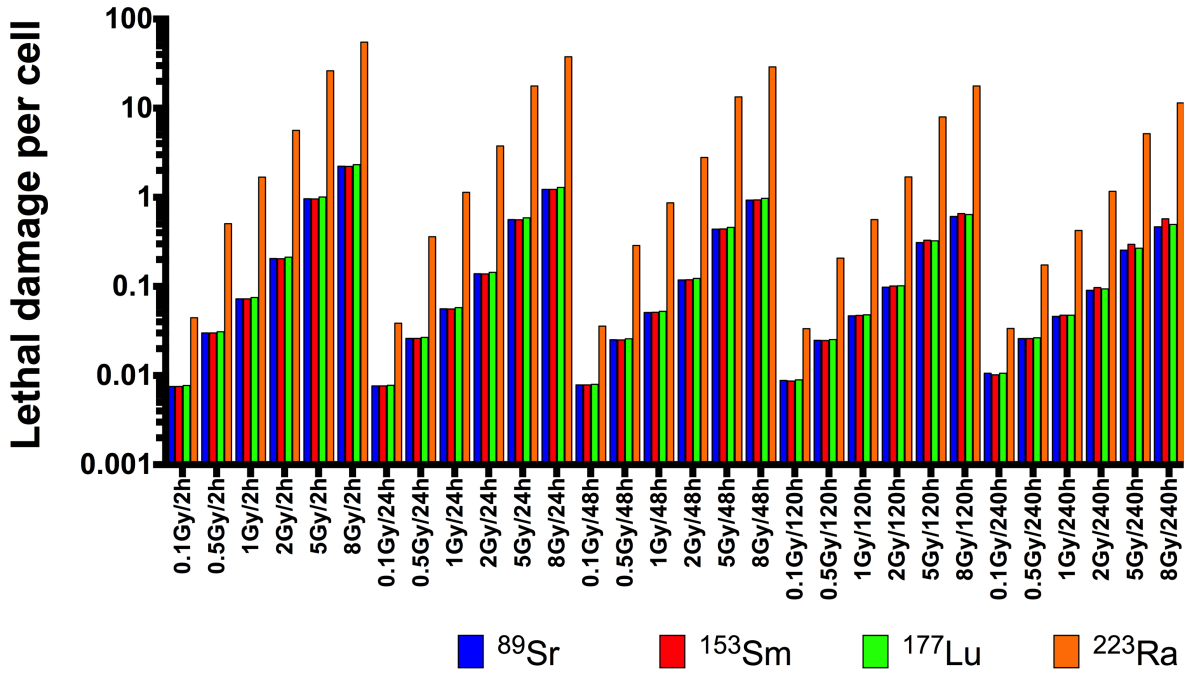


**Figure 5:** Average number of direct lethal damages per surviving cell after irradiation with distinct particles and different irradiation scenarios in a logarithmic scale.